



Supplement of

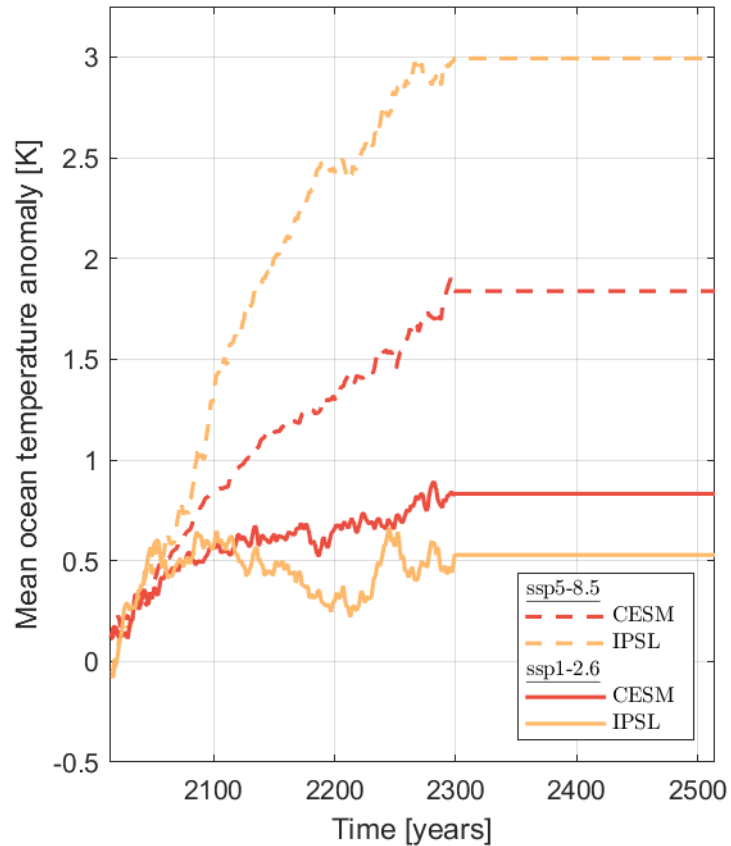
Approximating 3D bedrock deformation in an Antarctic ice-sheet model for projections

Caroline J. van Calcar et al.

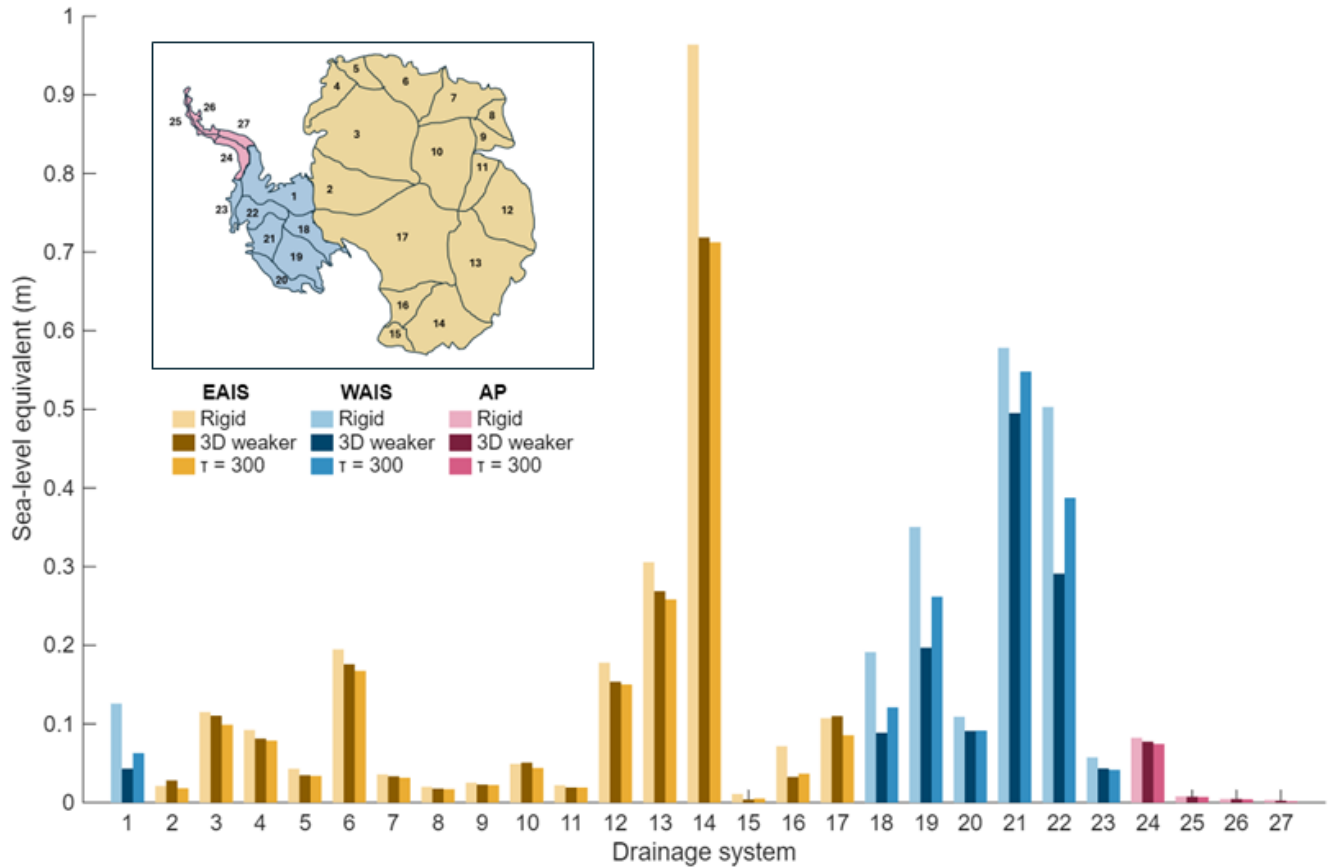
Correspondence to: Caroline J. van Calcar (c.j.vancalcar@tudelft.nl)

The copyright of individual parts of the supplement might differ from the article licence.

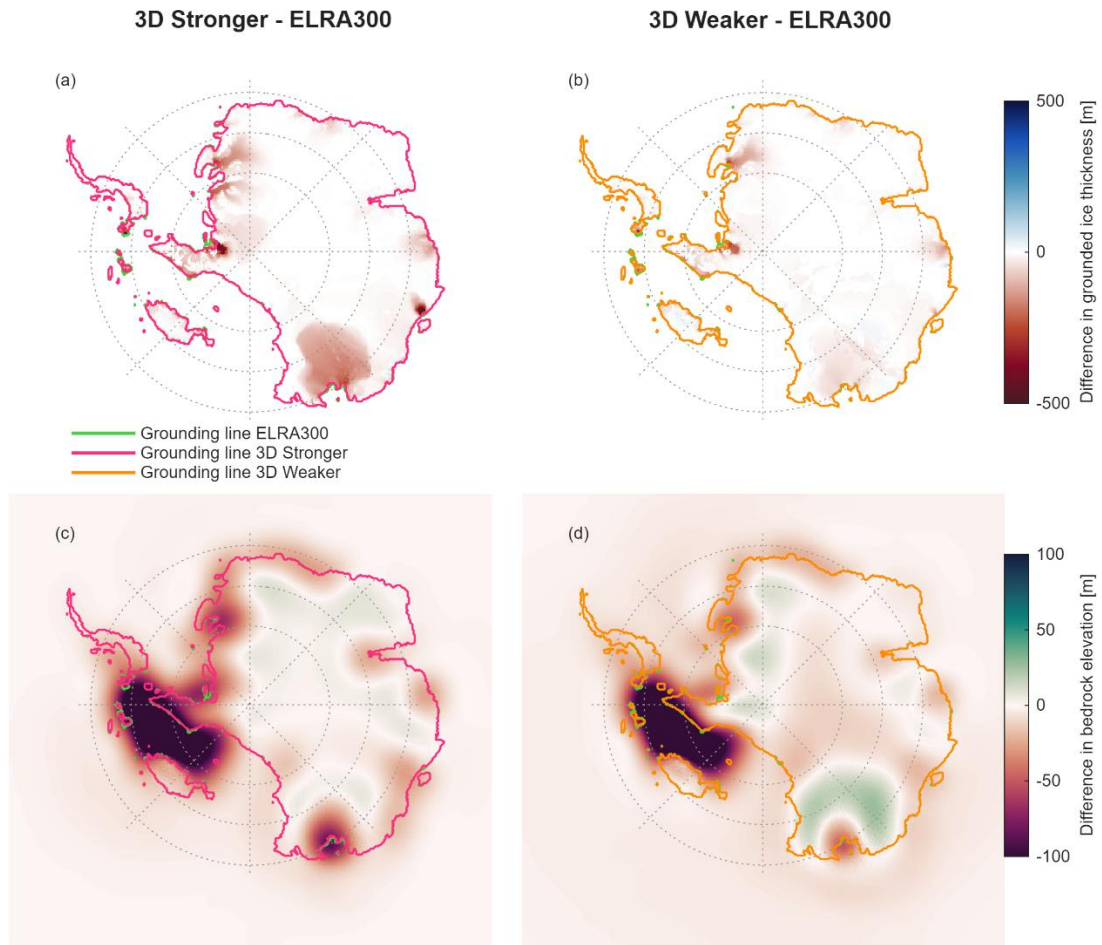
Supplements



5 **Fig. S1:** The mean ocean temperature anomaly over the present day ice shelf area between 2014 and 2514. The anomalies are taken from Coulon et al.9, who used ocean temperature anomalies from the global climate models CESM2-WACCM (indicated by CESM) and IPSL-CM6A-LR (indicated by IPSL) for two different IPCC scenarios: SSP5-8.5 and SSP1-2.6. The anomalies are averaged over the present day ice shelf area for each time step. Figure adopted from van Calcar et al. (2024).



10 **Fig. S2: Antarctic drainage systems 1–27, grouped into East Antarctica (yellow), West Antarctica (blue), and the Antarctic Peninsula (pink) following the basin definition of Zwally et al. (2012). For each basin, the accumulated barystatic sea-level contribution in 2500**



20

Fig. S3: Difference in accumulated grounded ice thickness above flotation (panel a and b) and bedrock elevation change (panel c and d) in 2500 between the ELRA model with a relaxation time of 300 years (referred to as ELRA300) and the two 3D Earth structures. Panels a and c correspond to 3D-stronger and panels b and d to 3D-weaker. The climate model IPSL is applied for the high emission scenario SSP5-8.5.

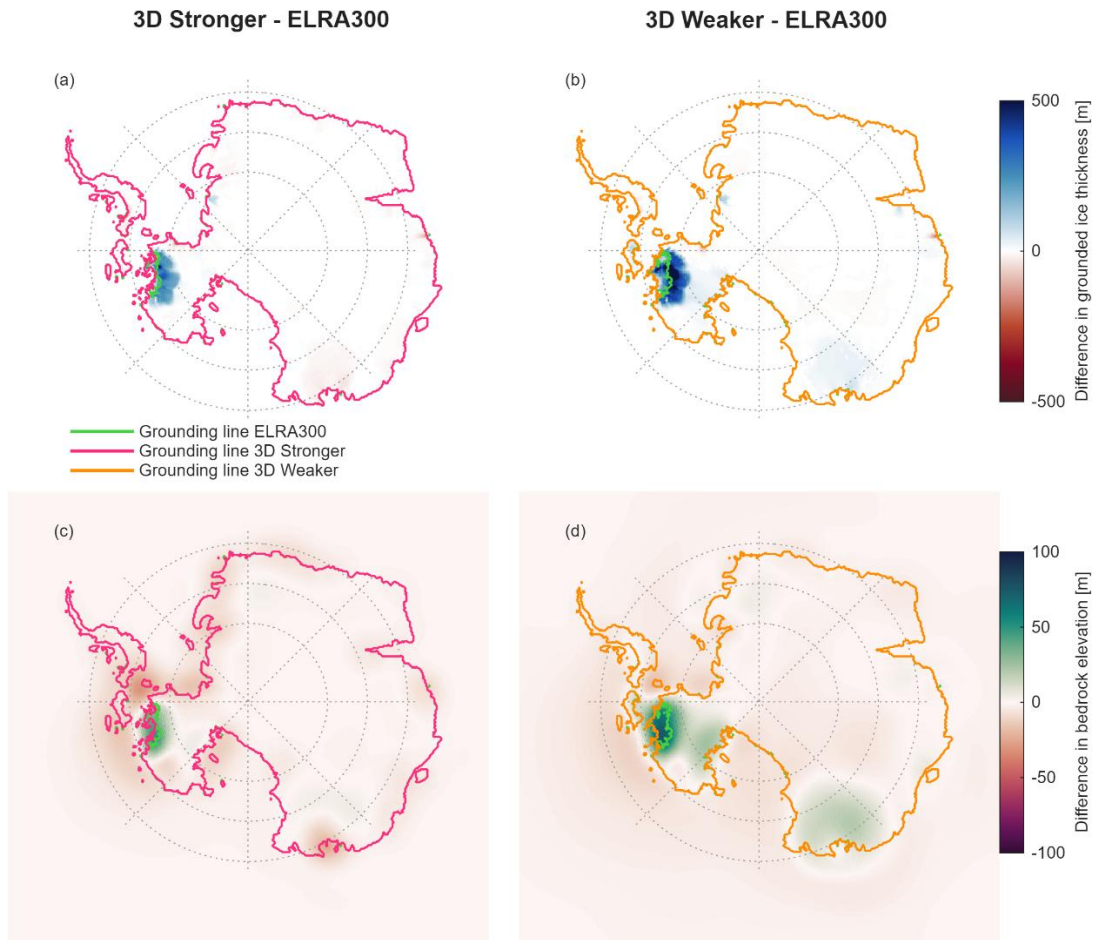


Fig. S4: Difference in accumulated grounded ice thickness above floatation (panel a and b) and bedrock elevation change (panel c and d) in 2300 between the ELRA model with a relaxation time of 300 years (referred to as ELRA300) and the two 3D Earth structures. Panels a and c correspond to 3D-stronger and panels b and d to 3D-weaker. The climate model IPSL is applied for the high emission scenario SSP5-8.5.

3D Stronger - ELRA300

3D Weaker - ELRA300

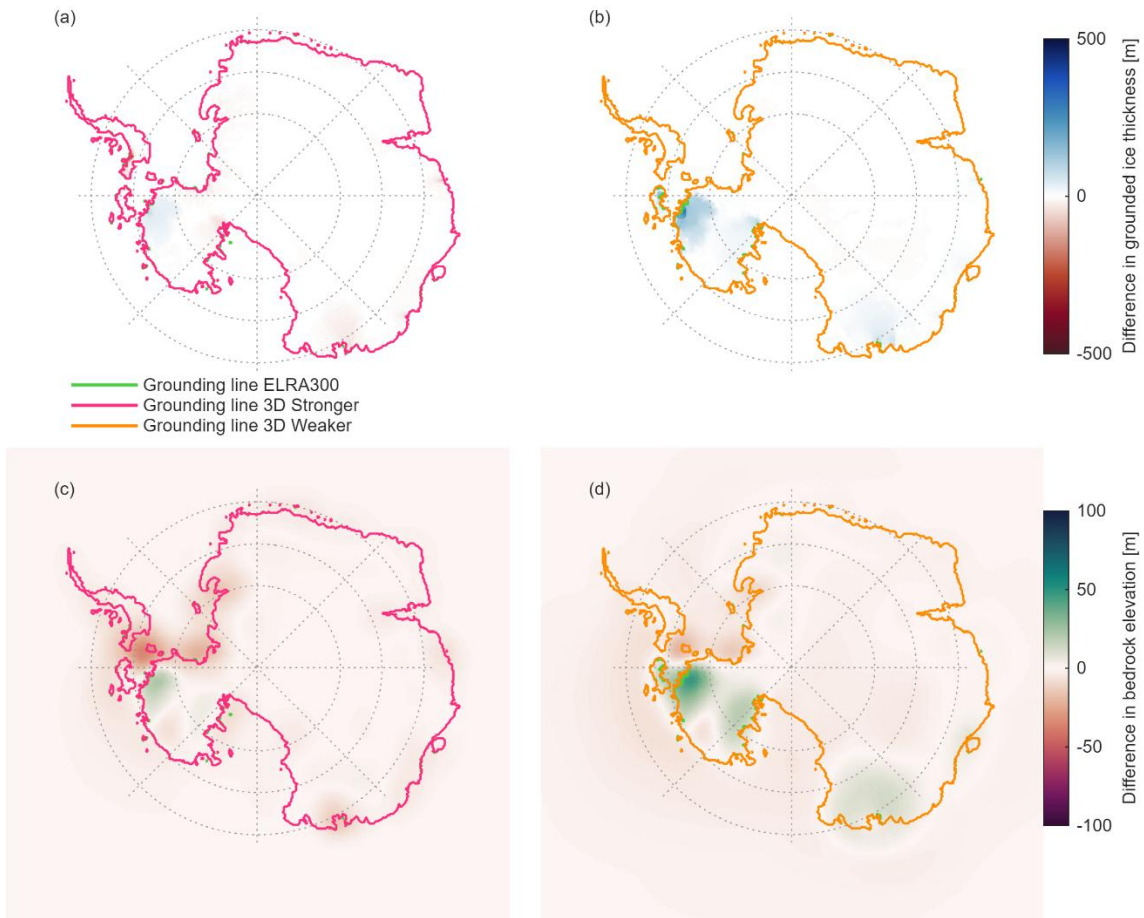
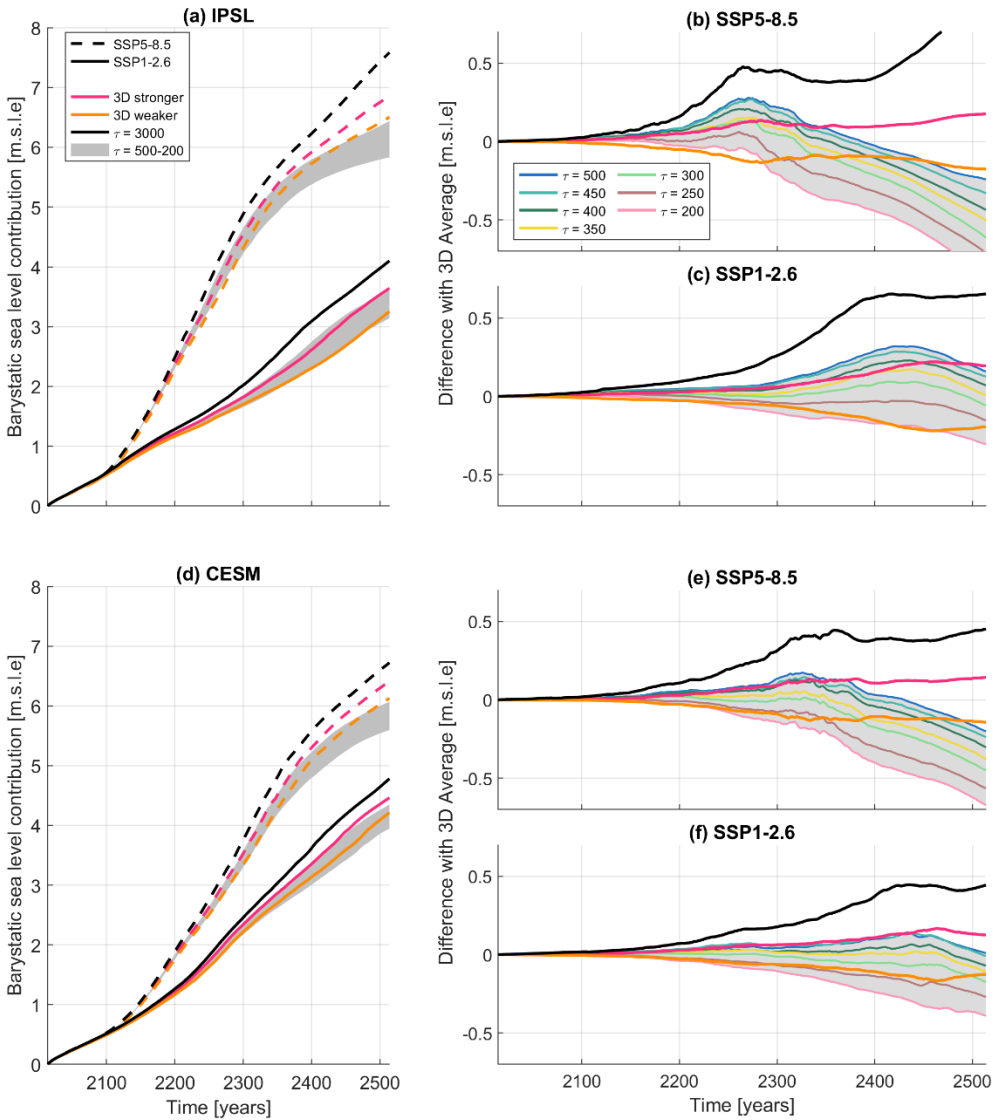


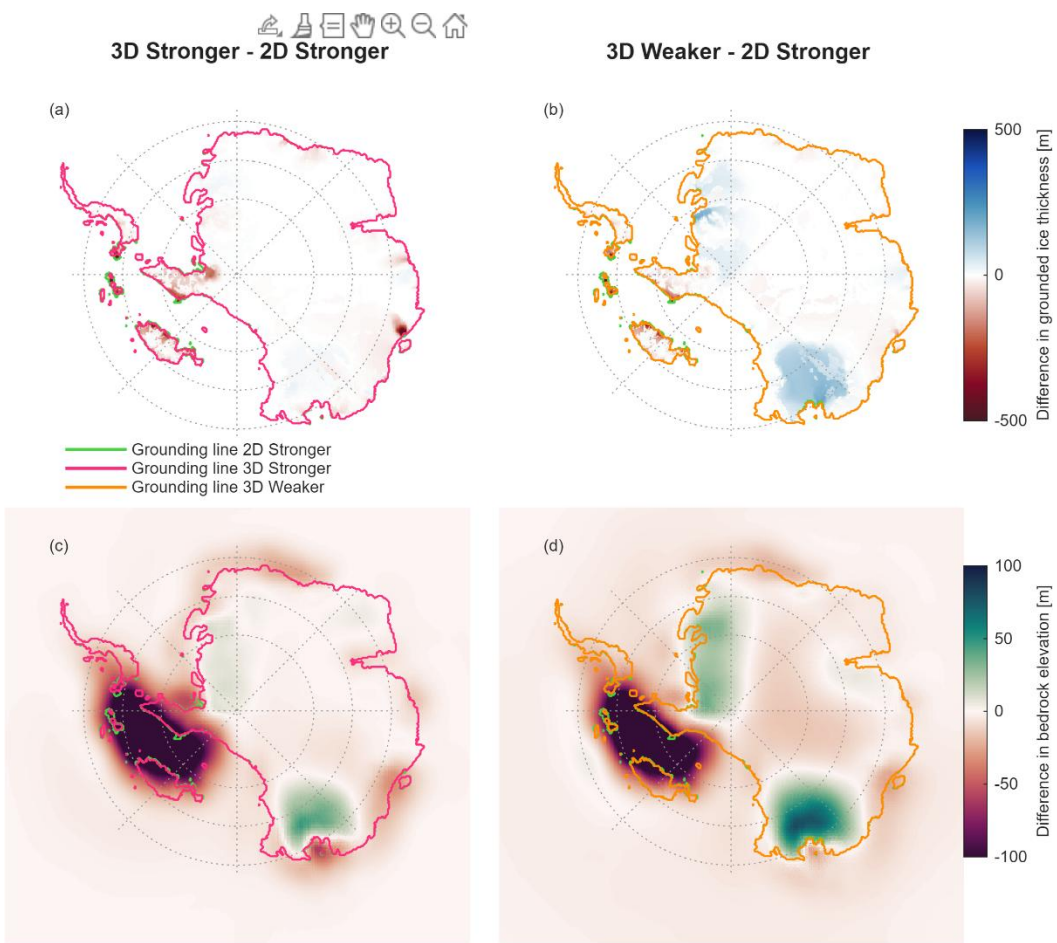
Fig. S5: Difference in accumulated grounded ice thickness above floatation (panel a and b) and bedrock elevation change (panel c and d) in 2300 between the ELRA model with a relaxation time of 300 years (referred to as ELRA300) and the two 3D Earth structures. Panels a and c correspond to 3D-stronger and panels b and d to 3D-weaker. The climate model CESM is applied for the high emission scenario SSP5-8.5.

30



35 **Fig. S6: The Antarctic ice sheet contribution to barystatic sea level rise using the 3D GIA model and the ELRA model for a high and a low emission scenario and two different climate models, IPSL-CM6A-LR (panel a) and CESM2-WACCM (panel d). Two different Earth structures are applied in the 3D GIA model, a stronger Earth structure and a weaker Earth structure. The relaxation time of the ELRA model is varied between 200 and 500 years, and a reference run of 3000 years is used. The flexural rigidity of $1.92 \cdot 10^{24} \text{ km} \cdot \text{m}^2 / \text{s}^2$ roughly corresponds to a lithospheric thickness of 60 km. Panels b, c, e, and f show the difference in barystatic sea level contribution between the ELRA model with different relaxation times and the average sea level contribution of the two 3D GIA simulations.**

40



45 **Fig. S7: Difference in accumulated grounded ice thickness above floatation (panel a and b) and bedrock elevation change (panel c and d) in 2500 between the LVELRA model with the 2D-stronger structure, a flexural rigidity corresponding to a lithospheric thickness of 120km and based on the average viscosity (Eq. 6) and the two 3D Earth structures. Panels a and c correspond to 3D-stronger and panels b and d to 3D-weaker. The climate model IPSL is applied for the high emission scenario SSP5-8.5.**

3D Stronger - 1D19

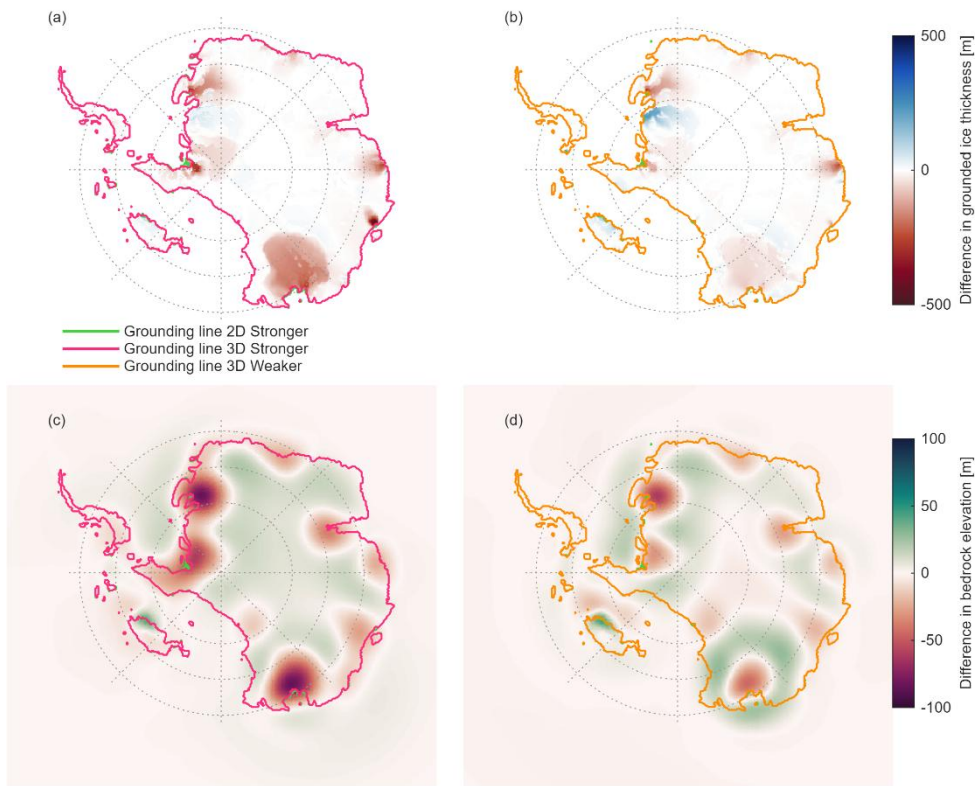


Fig. S8: Difference in accumulated grounded ice thickness above floatation (panel a and b) and bedrock elevation change (panel c and d) in 2500 between 1D19 and the two 3D Earth structures. Panels a and c correspond to 3D-stronger and panels b and d to 3D-weaker. The climate model IPSL is applied for the high emission scenario SSP5-8.5.

55

Tab. S1: Root mean square error [m] of the difference between the sea level change using ELRA with a uniform relaxation time and the average sea level change of the two 3D GIA simulations. The relaxation time with smallest root mean square error, considered as the optimal choice, is highlighted in green.

Relaxation time [yr]	3000	500	450	400	350	300	250	200
CESM585	0.29	0.1	0.08	0.08	0.08	0.09	0.12	0.2
CESM126	0.24	0.11	0.09	0.05	0.03	0.02	0.05	0.11
IPSL585	0.37	0.14	0.13	0.12	0.12	0.15	0.19	0.24
IPSL126	0.4	0.21	0.18	0.16	0.14	0.08	0.04	0.03
Total	1.31	0.55	0.49	0.41	0.37	0.35	0.39	0.58

60

65 Tab. S2: Root mean square error [m] of the difference between the sea level change using LVELRA and the average sea level change of the two 3D GIA simulations. Equation 8 in the main text is used to derive the 2D relaxation time maps based on two different 3D Earth structures and two different fitting methods to fit the relaxation time to viscosity. The sea level contribution is computed using ELRA with a uniform lithospheric thickness of ~120 km and ~60 km. The configuration with smallest root mean square error, considered as the optimal choice, is highlighted in green.

3D Earth structures	Weaker	Weaker	Weaker	Weaker	Stronger	Stronger	Stronger	Stronger
Fitting method	Average	Average	Lower bound	Lower bound	Average	Average	Lower bound	Lower bound
Lithospheric thickness [km]	120	60	120	60	120	60	120	60
CESM585	0.29	0.45	0.08	0.16	0.05	0.11	0.09	0.07
CESM126	0.25	0.35	0.03	0.1	0.03	0.1	0.08	0.04
IPSL585	0.3	0.5	0.1	0.2	0.06	0.1	0.15	0.11
IPSL126	0.23	0.37	0.04	0.07	0.02	0.13	0.16	0.08
Total	1.06	1.67	0.24	0.53	0.17	0.44	0.49	0.3

Tab. S3: Root mean square error [m] of the difference between the sea level change using a 1D GIA model and the average sea level change of the two 3D GIA simulations. The viscosity profiles of the 1D Earth structures are shown in Fig. 1 in the main text. The 1D Earth structure with smallest root mean square error, considered as the optimal choice, is highlighted in green.

1D Earth structure	1D21	1D20	1D19	1DASE
CESM585	0.23	0.17	0.07	0.1
CESM126	0.2	0.15	0.05	0.04
IPSL585	0.28	0.21	0.11	0.15
IPSL126	0.32	0.27	0.02	0.03
Total	1.03	0.8	0.25	0.32

References

Zwally, H. J., Giovinetto, M. B., Beckley, M. A., and Saba, J. L.: Antarctic and Greenland drainage systems. GSFC, 265, 2012.